Stress evolution in multilayer polymer coating under thermal and pressure loading applied to the pipeline structure

M.R. Tchoquessi Diodjo, Y. Joliff, L. Belec, E. Aragon, F.X. Perrin

Stress evolution in multilayer polymer coating under thermal and pressure loading applied to the pipeline structure

M.R. Tchoquessi Diodjo [a], Y. Joliff [a,*], L. Belec [a], E. Aragon [a], F.X Perrin [a]

[a] *MAPIEM, Université de Toulon, Avenue Georges Pompidou, BP 56, 83957, La Garde, France*

[*] Corresponding author:
- Y. Joliff: joliff@univ-tln.fr

Abstract

Pipelines must have good mechanical properties during their service life. To improve this lifetime, a protection against corrosion is applied on the steel cylinder by coupling a passive coating with an active cathodic protection. Otherwise, it is well known that the presence of internal stresses in organic coatings is a current phenomenon which can result in the loss of adhesion. These phenomena can be critical for safety and lead to expensive maintenance operations. In order to identify areas of overstress and estimate the values reached in the pipeline, and especially in its coating, the development of numerical models appears relevant. The models show that significant stresses are present in the coating and at the different interfaces during the pipeline operation. Their values change with the different loading cases which can be encountered on the transportation network. From these results, the stress is essentially concentrated in the steel/coating interface with a maximal value lower than 10 MPa.

Keywords: Pipelines, organic coatings, internal stresses, disbanding, Finite Element Approach

Nomenclature

DMA	Dynamic Mechanical Analysis	α	Coefficient of thermal expansion
		Cp	Specific heat
FC	Safety coefficient	C1	Coefficient of viscoelasticity
FBE	Fusion Bonded Epoxy	C2	Coefficient of viscoelasticity
		ϕ	Diameter
MOP	Maximum Operating Pressure	E	Young's modulus
		e	Thickness
PE	Polyethylene	gi	Relaxation modulus
PPP	Polypropylene	J	Compliance
		λ	Thermal conductivity
R_e	Yield strength	ν	Poisson coefficient
		σ	Stress
WLF	Williams, Landel and Ferry law	ρ	Density
		T	Temperature
		t	Time
		τi	Relaxation time

1. Introduction

Thousands of kilometres of steel pipes are available to transport natural gas under pressure. Gas network consists of sections of pipes and related structures that fulfil specific functions in order to transport the fluids in optimal conditions. The injection stations constitute the entry points of the transport network. The compressor stations are evenly distributed along the transport networks to maintain the pressure and velocity of the gas in the pipelines. The delivery stations ensure the delivery of natural gas to manufacturers or downstream distribution networks. Delivery stations deliver natural gas to industrial companies or downstream distribution networks. These stations provide the functions of expansion, reheating, filtering or measuring gas.

There are many studies in the literature that investigate the durability of these systems in service [1, 2, 3, 4, 5, 6]. Most of these studies deal with the problems of corrosion [7, 8, 9, 10] or mechanical cracks but only a few are dedicated to the durability of the coating system. To improve the lifetime of the steel cylinder against the corrosion, a passive anti-corrosion coating system (Figure 1) is generally used in addition to cathodic protection [11, 12, 13, 14,

15].

Two types of coatings are mainly used. The first one, based on a single-layer system, consists in coating the steel cylinder with about 600 µm thick of epoxy layer (Fusion Bonded Epoxy FBE). This type of pipeline is mainly dedicated to American market. The second type of pipeline coating, used for the European market, is based on a three-layers system that associates a primer epoxy layer (Fusion Bonded Epoxy FBE), an adhesive polyethylene layer (PE Adhesive) and a polyethylene topcoat (PE Topcoat) [16]. The role of the FBE layer is to ensure an excellent adhesion between the steel substrate and the PE layer. This coating also allows good barrier properties. The PE Adhesive layer ensures an efficient link between FBE layer and PE Topcoat. The PE Topcoat allows a good chemical and mechanical resistances. The pipeline is manufactured by a semi-continuous process during which the steel cylinder is heated up to 200°C. The FBE layer is applied by spraying a powder at the surface of the heated steel cylinder. The PE Adhesive and PE Topcoat layers are then extruded on the latter. The pipeline then undergoes a rapid cooling in order to solidify the coating before storing at ambient air.

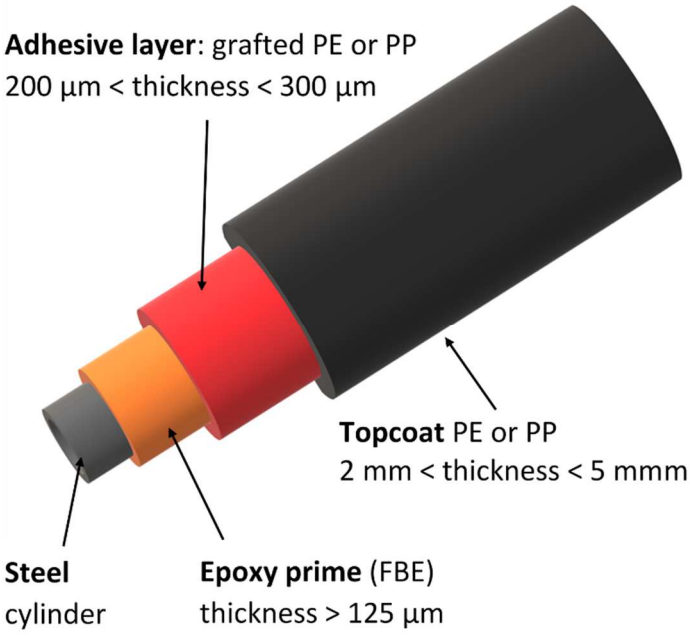

Figure 1: Thickness of three layers polyolefin coatings (FBE: Fusion Bonded Epoxy /PE: polyethylene / PP: polypropylene)

A number of negative feedbacks have been reported about a massive disbonding of the coating in the case of the three-layer coating in service since a few years [17, 18, 19]. This disbonding has been observed at the steel/coating interface without damage to the coating top surface. Moreover, no corrosion has been observed on the steel pipeline under these disbonding areas. Roche et al. [18] have concluded about a degradation of the Steel/FBE interface due to the water diffusion throughout the coating. If the diffusion of water molecules in the coating is a credible assumption, the rare cases of similar damage on new pipelines can hardly be explained. Moreover, to our knowledge, there has been no such case of reported damage on pipelines coated with monolayer epoxy systems while these systems are also sensitive to water diffusion. Legghe et al. [20], with a numerical approach, have estimated the internal stresses levels generated during the processing of monolayer and three-layer coated pipelines. Considering an elastic behaviour (more unfavourable case – without dissipation) in a first approximation, the authors obtain a large gap (x4) between stress levels in both systems. All these observations suggest that the stresses at the steel/coating interface generated during the coating pipeline process might cause the disbonding of the coating.

Some authors [21, 22, 23, 24] have estimated the stress in multi-layered coating. In the case of the pipeline coating [25, 26, 27, 28, 29, 30, 31, 32], this stress is usually due to the mismatch of thermal expansion coefficients of steel and polymer coating. Indeed, a longitudinal contraction can be observed after the pipeline coating process [18]. A similar result has been obtained by numerical simulation of the process with around 12 mm of coating contraction for a pipeline with a length of 20 m [33]. In a previous work [34], it has been shown that far from pipeline extremities, interfacial stress levels are less than 5 MPa at steel/epoxy interface and less than 16 MPa at epoxy/polyethylene interface. Moreover, in another study [35], the impact of the pipeline geometrical characteristics on the stress level was evaluated. It has been demonstrated that radial contraction increases linearly with increase of pipe diameter, which

is beneficial for adhesion of the coating. Moreover, whatever the size of the pipe, a stress around 5 - 7 MPa is calculated at the steel/epoxy interface. All these results converge to the existence of stresses at the interfaces. During the storage, the stress level will decrease due to the relaxation of the coating (Figure 2). After one year of storage, the residual stress at the steel/FBE interface (3MPa) is higher than the residual stress at the FBE/PE interface (2 MPa) [16].

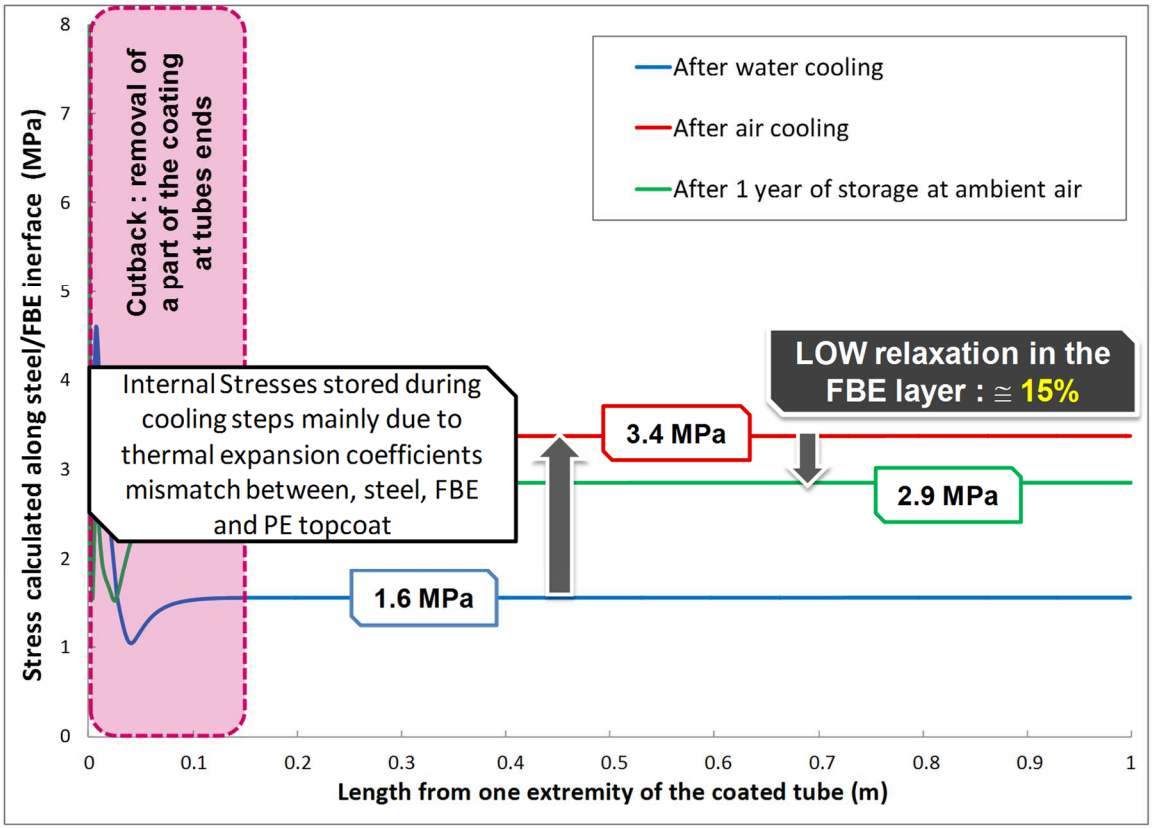

Figure 2: Evolution of the Tresca criteria along steel/FBE interface after the different types of cooling process and after 1 year of storage at ambient air [16]

If a residual stress is well identified at the steel/coating interface, its intensity cannot explain the damage observed on the pipeline. A possible cause of this disbonding could come from the coupling between this internal stress due to the process and the stress generated in operation (temperature and pressure). So, this paper proposes to continue this investigation on the quantification of the stresses in coated pipeline in service conditions by a finite element approach. In service, pipelines are buried in soils and transport more or less hot fluids under

pressure. Fraldi et al. [36] show that the mismatch of Young's moduli and Poisson ratios of a polymer multilayers promotes its delamination. So, the influence of internal pressure and service temperatures on the stresses in the three-layer coating will be investigated. Numerical models are compared to experimental data and industrial feedback.

2. Materials and method

The metal structure is designed to withstand the internal and external pressure acting on the structure. The thickness, diameter and grade of steel are determined according to the MOP criteria (Maximum Operating Pressure). This criteria is calculated from Equation 1 [37].

$$MOP = FC \times R_e \times \frac{2 \cdot e_{Steel}}{\phi_{Steel}} \quad \text{Equation 1}$$

where R_e is the yield strength of the grade of steel used, e_{Steel} and ϕ_{Steel} represent respectively the thickness and the nominal pipe (i.e. inside diameter) of the steel cylinder and FC is a safety coefficient which depends on class location of the pipe. For example, a site identified as category 1 corresponds to a cross-country gas pipeline (no sensitive equipment at proximity).

In this work, the geometry of one of the most common pipelines of the GRTgaz transport network is chosen. It is a steel tube with a wall thickness of 7.3 mm and an inside diameter of 602.7 mm. GDF SUEZ company recommends the use of steel with a yield strength of 383 MPa. These pipes are intended for operation at 72% of the yield strength of steel for class 1 location where the safety factor is equal to 0.72. In this case, according to Equation 1, the maximum operating pressure is equal to 6.6 MPa.

Furthermore, natural gas is transported through gas pipelines at temperatures between -20 °C and +60 °C. The gas temperature and soil temperature will be considered for the determination of interfacial stresses. Three cases will be considered: two extremes cases

where gas temperature is either -20 °C or +60 °C and soil temperature is +20 °C, and a most common case where gas and soil are at the same temperature of +15 ° C (Table 1).

Table 1: Three thermal parameters considered

	Case (a)	Case (b)	Case (c)
T_{soil} (°C)	20	15	20
T_{gas} (°C)	-20	15	60

2.1. Numerical model (Finite element method - FEM)

A commercial Finite Element Analysis software, Abaqus™ [38], is used in this work. The properties of the PE Adhesive and PE Topcoat layers being similar, the thickness of the adhesive layer will be added to the thickness of the PE Topcoat in the models. The numerical model is based on an axisymmetric representation to describe the pipeline structure. It has been previously shown that only 1 meter of pipeline length can be considered for the numerical models [33]. A coupled thermomechanical calculation is realized to describe the problem. A study of the convergences of the various mesh elements (quadrangle ou triangular) was made in advance of this work [39]. Each part has been meshed from quadrilateral elements with a linear interpolation (4 nodes) and a reduction of integration points (element type CAX4RT). The mesh is built using the "Structured" technique. The boundary conditions applied on the pipeline are detailed in Figure 3. An internal pressure equal to 6.6 MPa (MOP value from Equation 1) is applied to the inner surface of the pipe (blue arrows in Figure 3). This study considers a buried pipeline. External pressure is neglected in this work. Three temperature conditions are imposed on the internal surface of the metal cylinder in contact with the gas (red line in Figure 3) and on the top surface coating in contact with the soil (yellow line in Figure 3). A perfect contact (Tied – green lines in Figure 3) is assumed between the different layers of coating and the steel pipe. No debonding

can appear during the simulation for any interface. A total transmission of the thermal and the mechanical properties from one material to another one is allowed.

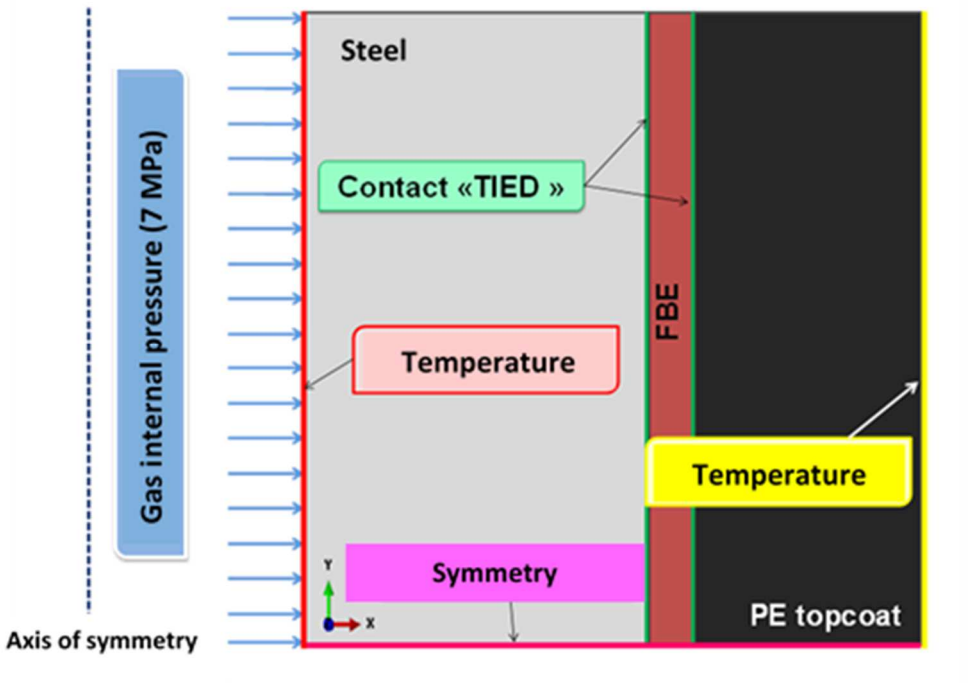

Inside diameter

Steel: 602.7 mm

Thickness

Steel: 7.3 mm

FBE: 200 µm

PE: 3.6 mm

Figure 3: Loading and boundary conditions applied on the pipeline

Considering the previous results [16, 34, 35], the model based on the thermo-viscoelastic behaviour is the most performing and it has been chosen for this study.

With ABAQUS™ software, materials viscoelasticity can be modelled either by introducing normalized parameters stemming from relaxation tests, or by using the generalized Maxwell model described by a series of exponentials named Prony series. The generalized Maxwell model is the most general form of the linear model for viscoelasticity. This model considers that relaxation in a polymer cannot be described by a single characteristic time, but by a distribution of times associated to the distribution of molecular chain length segments with different molecular mobilities. It is then assumed that shorter ones contribute less than longer ones, which induces the time distribution. The generalized Maxwell shows this by having as many spring–dashpot Maxwell elements as necessary to represent accurately the distribution. Each spring is characterized by an elastic modulus and each dashpot by a viscosity ηi. Here,

g_i is a dimensionless elastic modulus, normalized by the instantaneous elastic modulus g_0. g_i and η_i are used to define the relaxation time $\tau_i = \eta_i/g_i$.

ABAQUS™ software was then used to determine the parameters of Prony series using a non linear least square method to fit properly experimental relaxation curves [16].

Williams, Landel and Ferry proposed an empirical equation (WLF law) which gives an equivalence between time and temperature (Equation 1). T represents the temperature, T_{ref} is the reference temperature (glass transition temperature or operating temperature for example). C_1 and C_2 are empirical constants.

$$log(a_T) = \frac{-C_1(T-T_{ref})}{C_2+(T-T_{ref})} \quad (1)$$

The principle of time-temperature equivalence states that the passage from Tref to T amounts to multiplying the time scale by a thermal shift factor $a_{T \rightarrow Tref}$ which depends only on T and T_{ref}. Thus, there is a relation between compliance at the reference temperature and compliance at the temperature considered: J (t, T_{ref}) = J (t x $a_{T \rightarrow Tref}$, T). By a suitable transformation of the abscissa scale, for each temperature, we can obtain the superposition of the curves. Constants C_1 and C_2 are adjusted so that Equation 1 is verified.

Input data for simulation are specified in Table 2, Figure 4, Figure 5, Table 3 and Table 4. These values come from experimental measurements or from the literature [40].

Table 2: Thermal and mechanical parameters used in the models

Materials	λ (W.m^{-1}.K^{-1})	ρ (kg.m^{-3})	E (GPa)	ν	α (K^{-1})	Cp (J.kg^{-1}.K^{-1})
Steel	21 (a)	7800 (a)	210 (a)	0.30 (a)	12x10^{-6} (a)	650 (a)
FBE	0.35 (a)	1400 (a)	f(T) (b)	0.33 (a)	24x10^{-6} (a)	f(T) (c)
PE	0.63 (a)	955 (a)	f(T) (b)	0.42 (a)	175x10^{-6} (a)	f(T) (c)

with λ thermal conductivity, ρ density, E Young's modulus, ν Poisson coefficient, α Coefficient of thermal expansion and Cp specific heat (a) from literature [40], (b) by dynamic mechanical analysis tests, (c) by modulated differential scanning calorimetry tests

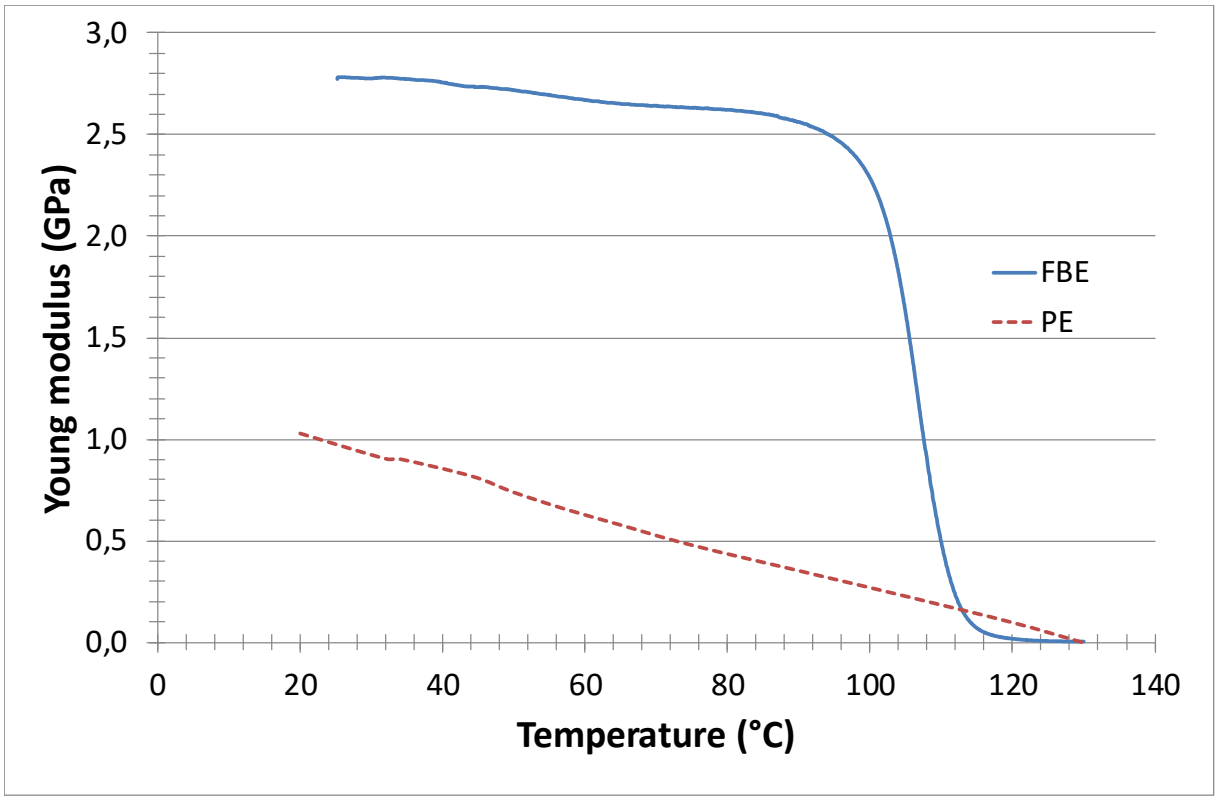

Figure 4: Young modulus as a function of temperature for polyethylene and epoxy (DMA at 1 Hz in shear mode in linear viscoelastic range)

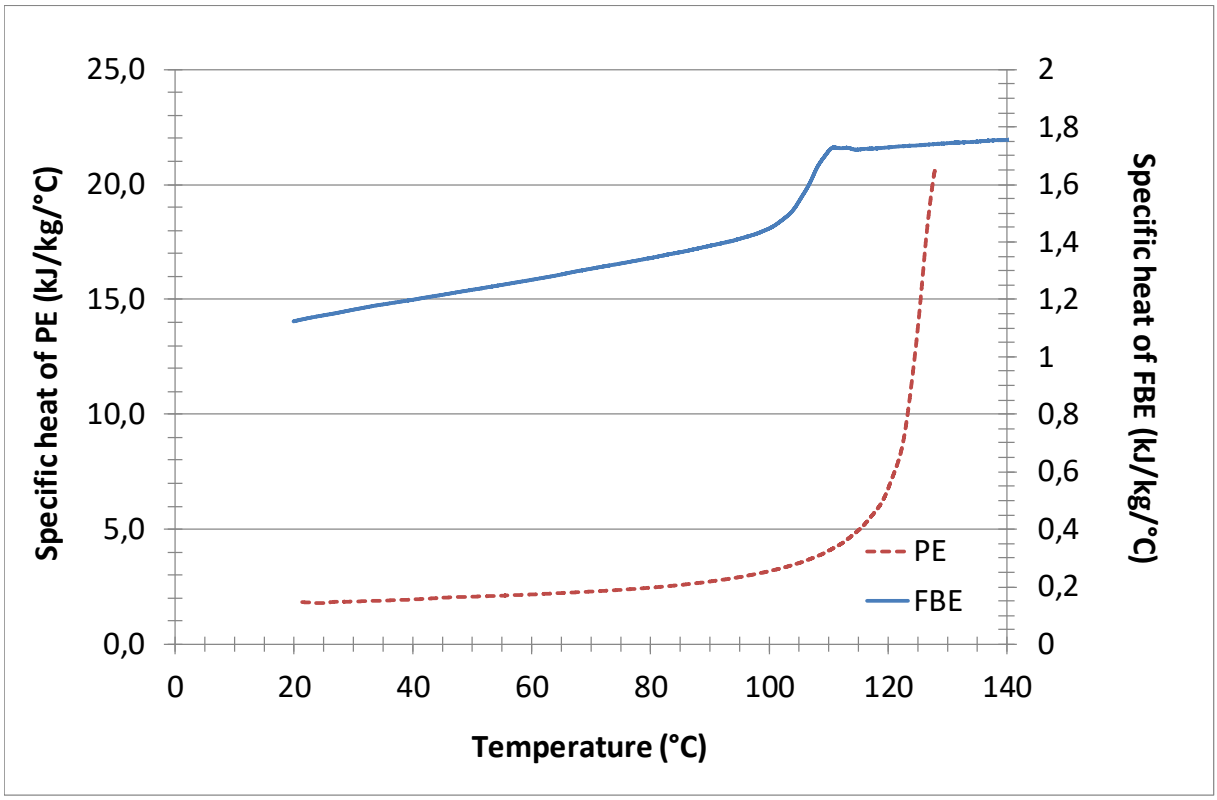

Figure 5: Specific heat as a function of temperature for polyethylene and epoxy (MDSC at 2 K/min)

Table 3: WLF parameters of PE and FBE used for the thermo-viscoelastic model [30]

Materials	T_{ref} (°C)	C_1	C_2
FBE	100	12	50
PE	25	16.4	112

with T temperature, C_1 and C_2 Coefficient of viscoelasticity

Table 4: Numerical parameters of the Prony series to describe the relaxation of PE and FBE at room temperature

Materials	Parameters of the Prony series (order 3)	1	2	3
PE	g_i	0.3	0.26	0.22
	τ_i	30	1000	1.5
FBE	g_i	0.06	0.064	0.094
	τ_i	1500	10000	100

The internal stress generated after one year of storage in ambient air at +20°C has been imported into the numerical model as the initial state of stress [16]. The very small deformations induced after the relaxation process during the storage period are neglected in this simulation. The deformation calculated in the radial and longitudinal directions does not exceed 0.05%.

3. Results

3.1. Temperature distribution

Figure 6 shows the temperature distribution in the three-layer coating in service condition for the three temperature conditions considered (Table 1).

PE and FBE are good thermal insulators [41] while steel is a good thermal conductor [42]. When gas and soil temperatures differ, a strong thermal gradient is generated between the steel internal surface in contact with the gas and the polyethylene outer surface in contact with the soil (Figure 6 a and Figure 6 c). On the other hand, when the gas and soil temperatures have the same value, a uniform temperature is logically calculated in the pipeline (Figure 6 b).

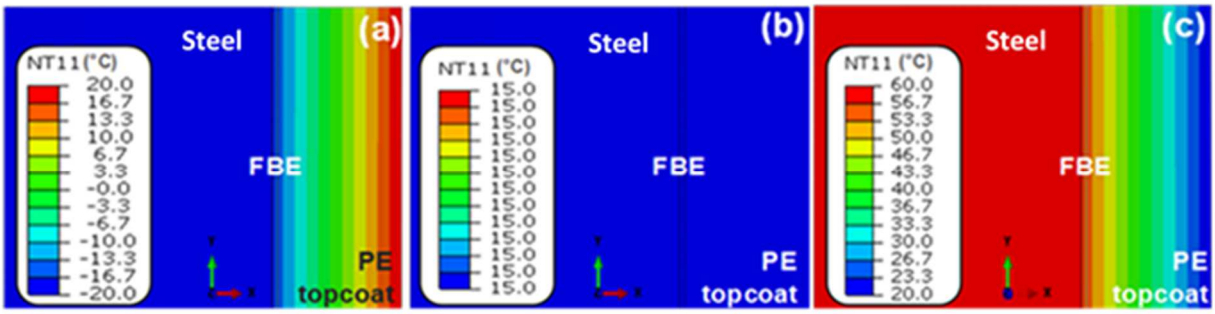

225

226 **Figure 6: Temperature isotherms in the pipeline for the 3 cases of thermal conditions considered in**
227 **Table 1**

228 Figure 7 represents the temperature evolution in the pipeline thickness for the three cases
229 studied. In case (a) where the internal temperature of the gas is -20°C and the soil temperature
230 is +20°C, the temperature of the steel cylinder varies slightly (between -20°C and -18°C). The
231 steel pipe is practically at the same temperature as the transported fluid. The temperature of
232 the thin FBE insulating layer varies between -18°C and -16°C and the thermal gradient of the
233 thick polyethylene insulating layer is even more marked with a temperature ranging from -
234 16°C (on the inner surface in contact with the FBE) and +20 °C (on the external surface in
235 direct contact with the soil). In case (b), where the gas and soil temperatures are equal to
236 +15°C, the temperature is the same throughout the thickness of the coated pipeline. As the
237 case (a), in the case (c) where the internal temperature of the gas is +60°C and the soil
238 temperature is +20°C, the temperature of the metal structure varies slightly between +60°C
239 and +58°C. The temperature of the FBE layer varies between +58°C and +55°C and a strong
240 thermal gradient between +55°C and +20°C is observed in the thick layer of polyethylene.
241 The same temperature gradient is calculated over the entire length of the pipeline.

242

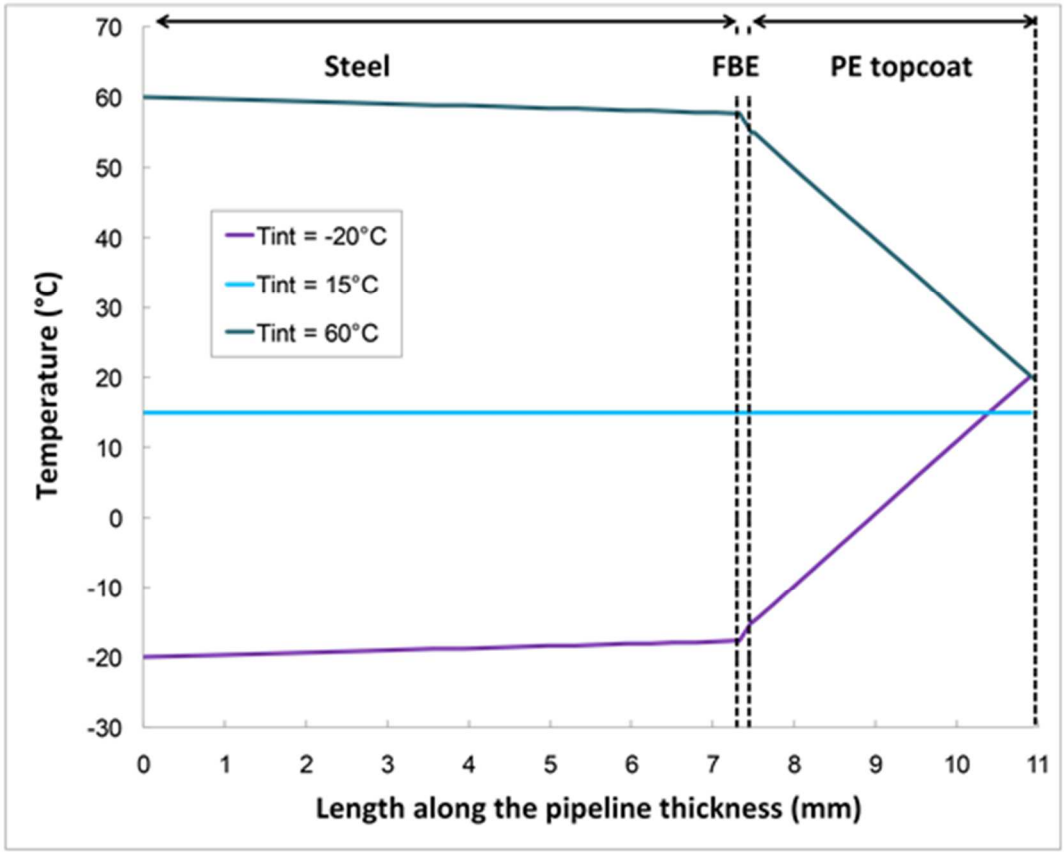

Figure 7: Evolution of temperatures along the pipeline thickness in service with an internal temperature of -20°C (case a), +15°C (case b) and +60°C (case c)

3.2. Stress distribution

The pipeline network consists of pipes placed end to end and assembled by welding. The assembly of the pipes by welding operation requires to be able to achieve a weld on the whole thickness to ensure a mechanical continuity of the assembly. To achieve this, a bevel (commonly named as “cutback) is made at the end surfaces of the elements to be assembled prior to welding them together [34]. The mechanical operations of removing the coating at the ends of the pipe should modify the stress state at the edges of the three-layers assembly. These phenomena have not been taken into account in this work. Therefore, we will focus on the stresses away from the end of the pipe.

Figure 8 presents the stress isovalues based on the Von Mises criterion and the stress isovalues in the circumferential direction (S33) (i.e. direction where the internal pressure is

applied). As expected, the internal pressure is mainly supported by the steel pipe.

In service, the maximum stress calculated in the steel cylinder according to the Von Mises criterion is equal to 290 MPa, 287 MPa or 286 MPa, when the internal temperatures of the gas are respectively set at -20°C., +15°C. or +60°C (Figure 8 a, b, c). In all cases, the maximum stress calculated according to the Von Mises criterion represents approximately 75% of the yield strength of the steel (383 MPa).

Furthermore, in the location category 1, at the MOP, the metal structure is sized for maximum stress on the steel pipe at 72% of its yield strength. This restriction is in good agreement with the numerical results which calculate a maximum stress of the metal structure at 75% of its yield strength.

Figure 9 shows the isovalues of the stresses away from the ends of the coated pipe in the radial (S11) and longitudinal (S22) directions for the three cases of temperature considered.

In the radial direction, the pressure due to the gas on the inner surface of steel cylinder generates compressive stresses in the three-layers coating, which vary linearly between -6.5 MPa (value at the inner surface of the steel cylinder in contact with the gas) up to -0.2 MPa (top surface of the steel cylinder in contact with the FBE). In the coating, the radial stresses are almost constant.

In the longitudinal direction, when the internal gas temperature is equal to -20 °C or +15 °C, the steel cylinder is in compression and the coating is in tension (Figure 9 d and e). When the internal gas temperature is equal to +60 °C, the steel cylinder is in tension and the coating is in compression (Figure 9 f). In all cases, the internal gas pressure applied on the steel cylinder generates shear stress at the interfaces and especially at the steel / FBE interface.

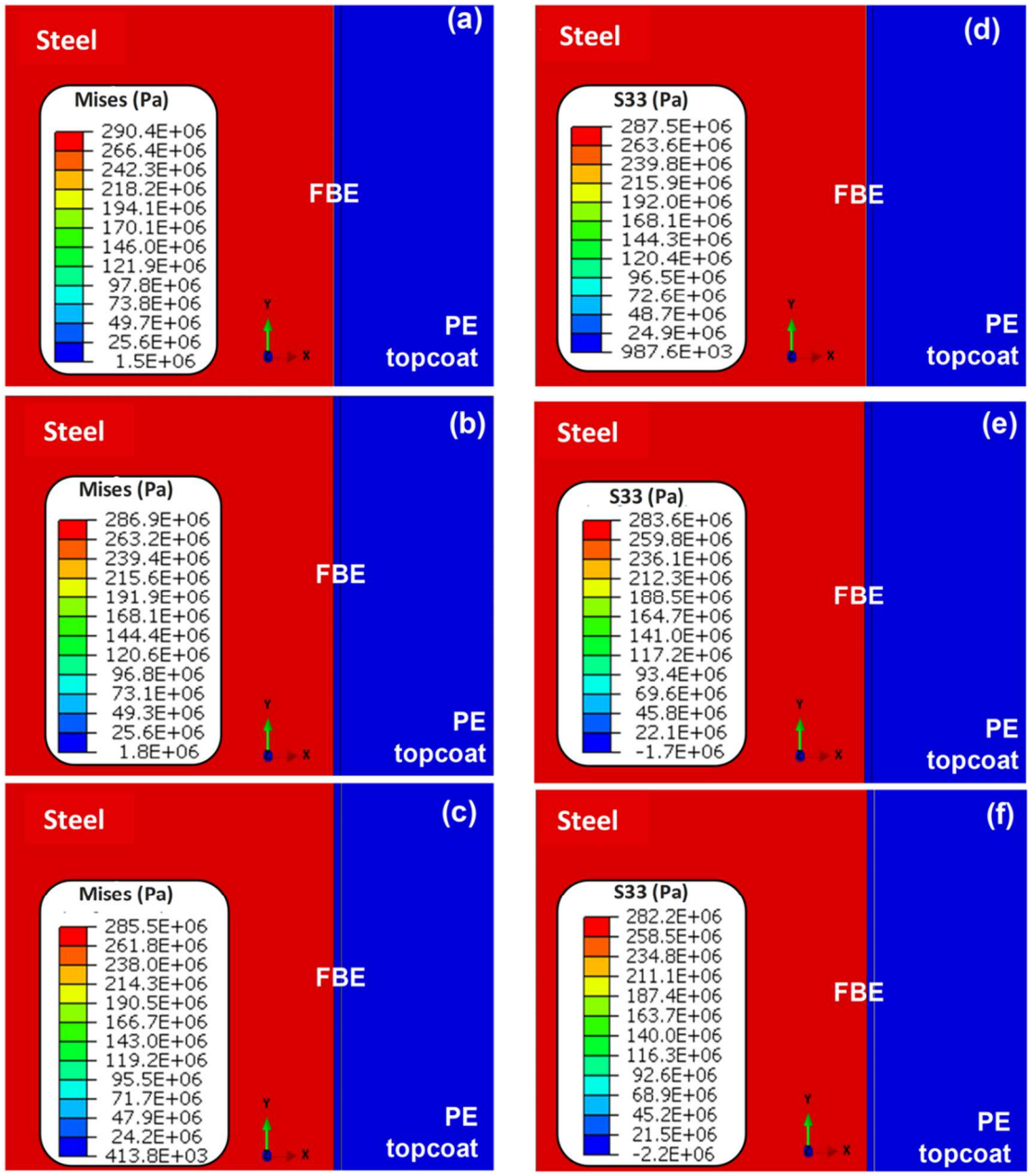

281

282 **Figure 8: Stress isovalues based on the Von Mises criterion (a,b,c) and stress isovalues in the circumferential direction**
283 **(d,e,f) calculated in case where the gas temperature is (a, d) -20° C, (b, e) +15° C and (c, f) +60° C**

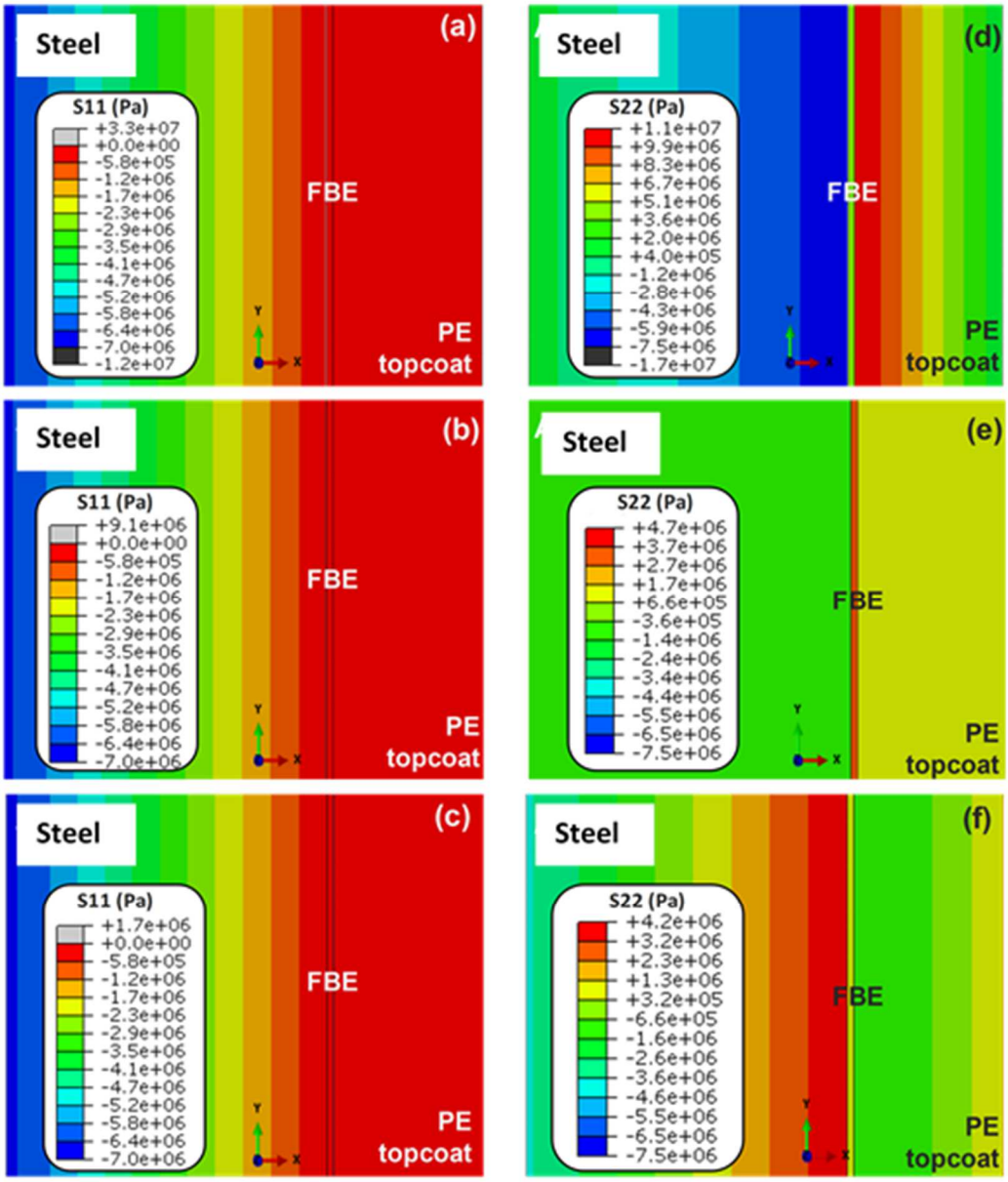

Figure 9: Radial (S11) (a,b,c) and longitudinal (S22) (d,e,f)stress isovalues calculated when gas temperature is (a,d)-20° C, (b, e) +15° C and (c, f) +60° C

As shear phenomena are mainly present at the interfaces, the Tresca criterion has been chosen to follow the stress evolution along the interfaces. It is important to remember that the classical criteria, as Von Mises or Tresca, are understood to be appropriate for pressure-insensitive materials (as steels for example), the pressure-sensitivity (in fracture, damage and yielding) of polymers often requires more advanced equivalent stress measures (as Drucker-Prager for example). Figure 10 and Figure 11 describe the evolution of the stresses calculated

according to the Tresca criterion at the steel/FBE interface and at the PE/FBE interface respectively.

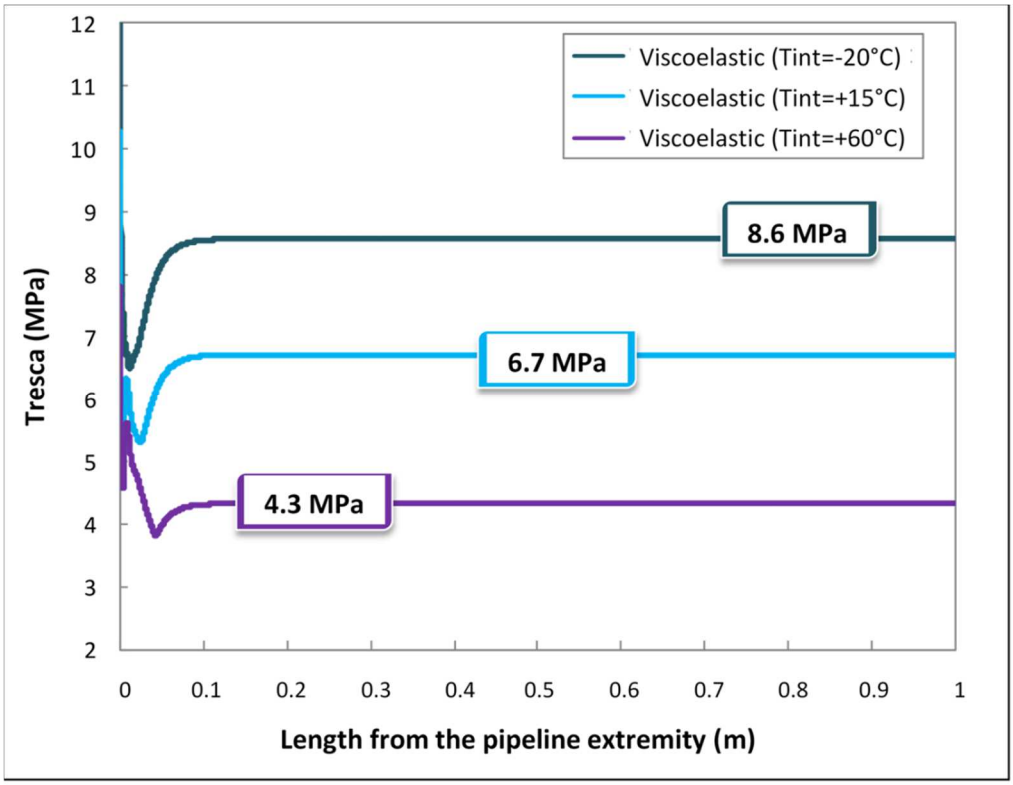

Figure 10: Evolutions of the stresses calculated in the FBE layer along the steel / FBE interface on a pipeline coated in service with an internal gas temperature of -20° C, +15° C or +60° C

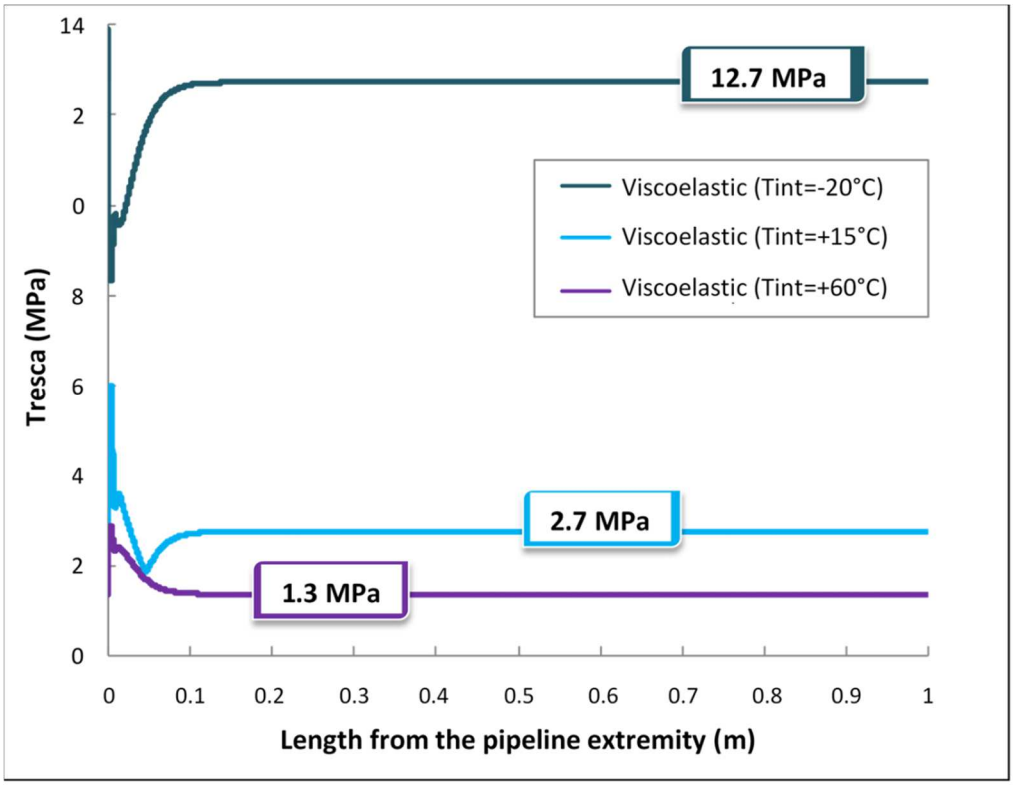

Figure 11: Evolutions of the stresses calculated in the PE layer along the PE / FBE interface on a pipeline coated in service with an internal gas temperature of -20° C, +15° C or +60° C

In the three cases studied, the internal pressure generated on the steel cylinder is the same. However, the thermal environments are different. The numerical results show that the most critical temperature distribution is calculated when the internal gas temperature is -20°C and the soil temperature is +20°C. In this case, stresses are respectively 8.6 MPa and 12.7 MPa at steel/FBE and PE/FBE interfaces. Lower stress levels are obtained when the temperature of steel increases (decrease of the value of the differential thermal expansion between the different layers of the pipeline structure).

The stresses at steel/FBE and PE/FBE interfaces are respectively 6.7 MPa and 2.7 MPa when the internal temperature is +15°C. Stress values decrease up to 4.3 MPa and 1.3 MPa respectively, when the internal temperature of steel is at +60°C. Furthermore, when the temperature of steel is at +60°C, the temperature of the FBE layer varies between +58°C and +55°C and PE layer temperature varies between +55°C and +20°C. However, around +55°C,

316 the Young's modulus of the FBE is equal to 2.6 GPa (E_{FBE} = 2.9 GPa at room temperature).
317 The Young's modulus of PE varies from 1 and 0.7 GPa between +20°C and + 55°C. So there
318 is certainly an effect of the drop of polymer mechanical properties with the temperature.
319 When the gas temperature is greater than or equal to +15°C, the stresses at the steel/FBE
320 interface are always greater than the stresses at the PE/FBE interface. On the other hand,
321 when the gas is injected into the pipeline at low temperature and especially at - 20°C, the
322 stress levels are higher at the PE / FBE interface.
323 Figure 12 compares the calculated stress levels with the thermo-viscoelastic model at the
324 steel/FBE interface from manufacture to use in service conditions. The manufacturing of the
325 three-layer coating is simulated by cooling the assembly with water (step 1) and then with air
326 (step 2). The storage of the tube coated for one year in the ambient air takes into account the
327 stress relaxation with time (step 3). The operation is simulated with a pressure applied on the
328 inner surface of the steel cylinder and an internal temperature of steel fixed at -20°C, +15°C
329 or +60°C (step 4 a, b or c). The study always focuses on stress levels away from the end of the
330 pipe.

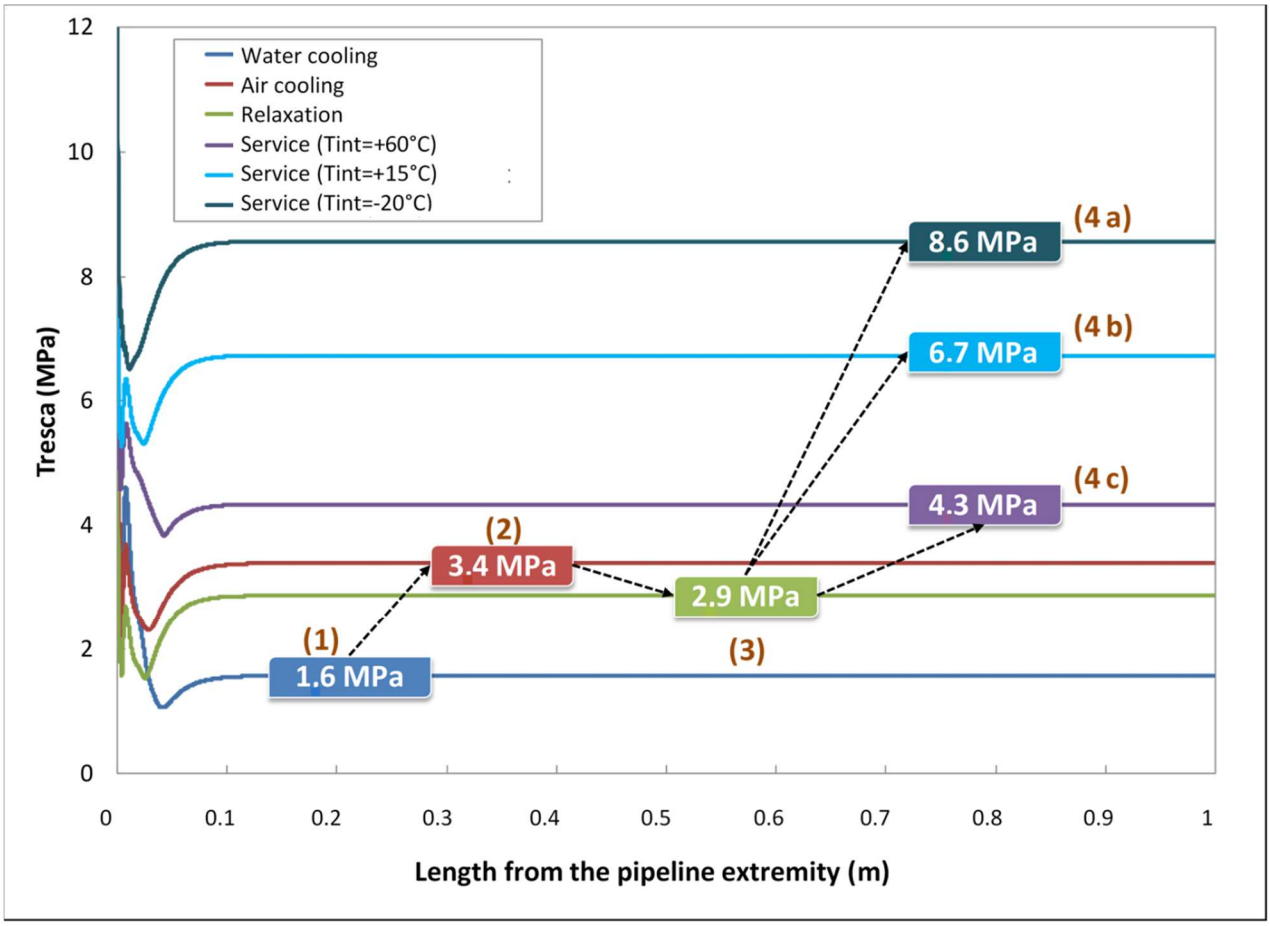

331

332 **Figure 12: Evolution of the stresses calculated according to the Tresca criterion at the steel / FBE interface during the**
333 **different stages of the pipeline life**

334 In agreement with the previous results [12,30], after the coating process, the stresses at the
335 steel/FBE interface increase from 1.6 MPa to 3.4 MPa due to the successive cooling stages
336 (water and air cooling). During one year of storage, a low relaxation of the FBE layer leads to
337 a slight decrease of the interfacial stress down to 2.9 MPa. In service, the gas pressure and
338 temperature gradients within the pipe result in increased shear stresses along the steel/FBE
339 interface. Stress can reach values greater than or equal to 4.3 MPa.

340 Similarly, Figure 13 compares the calculated stress levels from the thermo-viscoelastic model
341 in the PE/FBE interface at the different stages of the pipeline life.

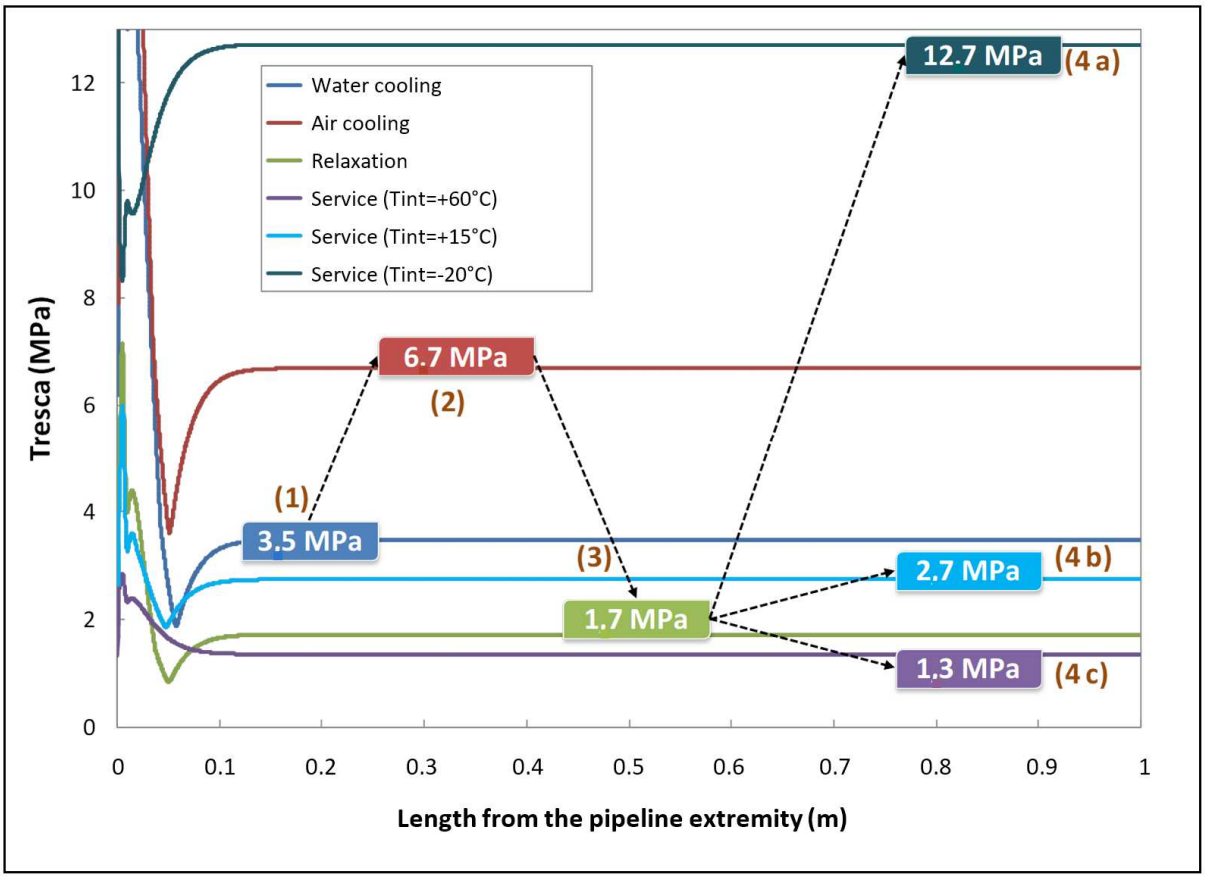

342

343 **Figure 13: Evolution of the stresses calculated according to the Tresca criterion at the PE / FBE interface during different**
344 **stages of the pipeline life**

345

346 As with the steel/FBE interface, the stress at the PE/FBE interface strongly increases from 3.5
347 MPa to 6.7 MPa during the cooling step. The high relaxation capability of polyethylene
348 allows a relaxation around 75% of the stresses generated in the PE layer. Finally, the stress is
349 only 1.7 MPa after one year of storage. According to the temperatures applied to the pipeline
350 in service conditions, the stresses at the PE/FBE interface may be lower or higher than the
351 residual stresses after one year of storage. In all cases, they are greater than or equal to 1.3
352 MPa.

353 When the internal temperature of the steel is equal to +60°C, the relaxation phenomena of the
354 PE are predominant and the stresses reach up to 1.3 MPa. On the other hand, when the
355 temperature of the injected gas is less than or equal to +15°C, shear stress developed at the
356 PE/FBE interface, becomes predominant and the stresses are then greater than those

calculated after one year of storage. They are respectively equal to 2.7 MPa or 12.7 MPa depending on the gas temperature (+ 15°C or -20°C). In service, when gas temperature is equal to - 20°C, the stresses become greater than the internal stresses generated by the coating process. It would be interesting to particularly monitor the condition of the coatings in these areas of the pipeline network in service. Nevertheless, these stresses remain much lower than the tensile strength of PE (35-40 MPa) [4] or the shear strength of PE (25-30 MPa) [5]. Until now, previous studies have concluded in a state of residual stress (post process) of a few units of MPa. However, Legghe [43] was demonstrated that the adhesion losses of the coating were directly correlated with the arrival times of water at the steel / FBE interface, with adhesions residuals of 2-10 MPa on rough substrates. The origin of the disbonding could come from the consequence of this loss of property in service and of a non-negligible state of internal stress.

4. Reliability of the numerical approach based on pipeline diagnostics

The internal stresses stored in the three-layer coating of a pipe in service for 6 years and with no adhesion between the coating and steel have been evaluated. A rectangular sample of three-layer coating has been cut in the longitudinal direction of the pipe (Figure 14). The planar sample is rapidly curved during storage at room temperature. This deformation is due to the presence of internal stresses stored in the coating during the process. Zhu et al. [42] have shown by image correlation and by finite element the curvature generated by the presence of a stress gradient in a multilayer material. Moreover, the generated curvature proves the presence of stress gradient in the coating. Figure 15 shows the deformed geometry of the sample 24 hours after cutting.

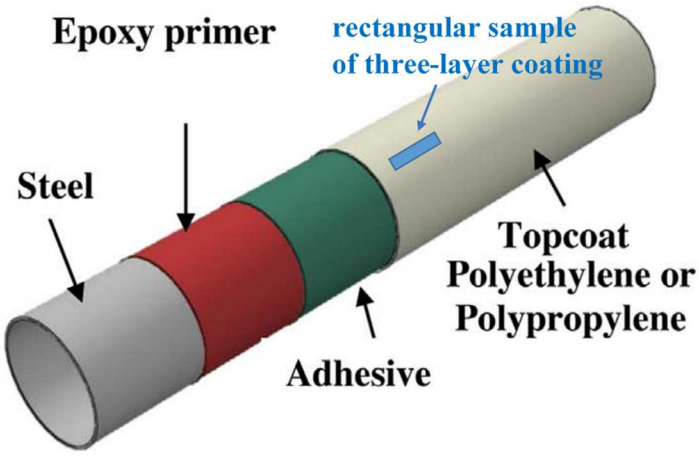

Sample dimensions:

Length: 175 mm

Width: 40 mm

Thickness: 3.8 mm

379 Figure 14: rectangular sample of three-layer coating cutted in the longitudinal direction of the pipe

380

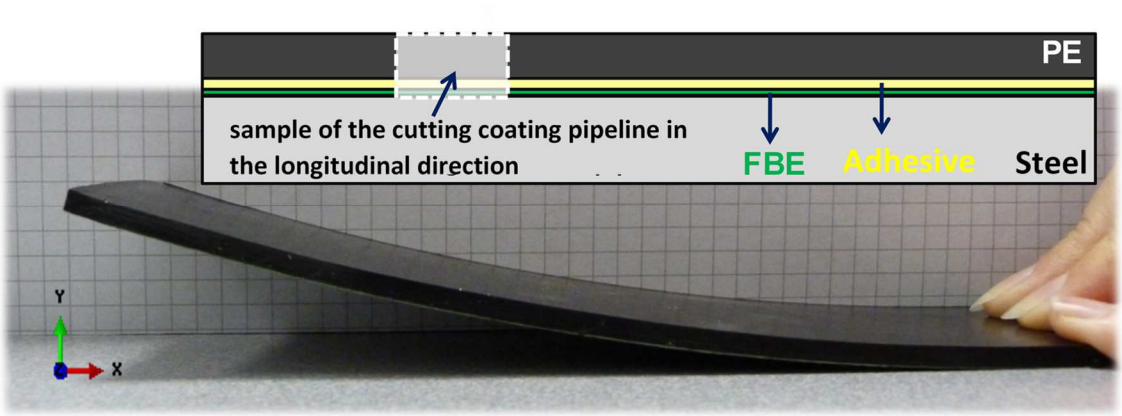

381

382 Figure 15: Visualization of the deformation in the coating 24h after cutting

383 In order to quantify these internal stresses, the geometry of the deformed coating is
384 reproduced in the ABAQUS™/standard solver. The objective is to simulate a return to the
385 planar shape of the curved sample and to quantify the stress associated with this operation. A
386 linear elastic approach is used to estimate the stress in the pipe coating in service.

387 ## 4.1. Model 1 based on mechanical loading

388

389 The numerical model developed is directly inspired by the numerical model used for stamping
390 process. In this case, a rigid tool will come and press the curved sample so that it regains a
391 planar shape (ie initial shape after the coating process). Numerical model is based on a

deformable part (coating curved) and 2 rigid parts (down and top tools – blue line Figure 16). The down rigid part is used as bearing surface for the sample, the second is used to apply a vertical displacement to the curved coating. Interactions between each solid part are managed by 2 contacts as described on Figure 16. A "surface to surface contact" has been chosen, with the assumption of perfect sliding properties between the tool surface and the surface coating. Isostatic boundary conditions - cancellation of degree of freedom to block the displacement of the sample without adding stresses, i.e. displacement of orange line $U_y = 0$ and displacement of a point of this line $U_x = 0$ - are imposed as shown in Figure 16. When one end of the curved coating is maintained on a plan surface, the other end is located at 33 mm from the plan surface. So, a displacement of -33 mm is therefore applied on top of the rigid part.

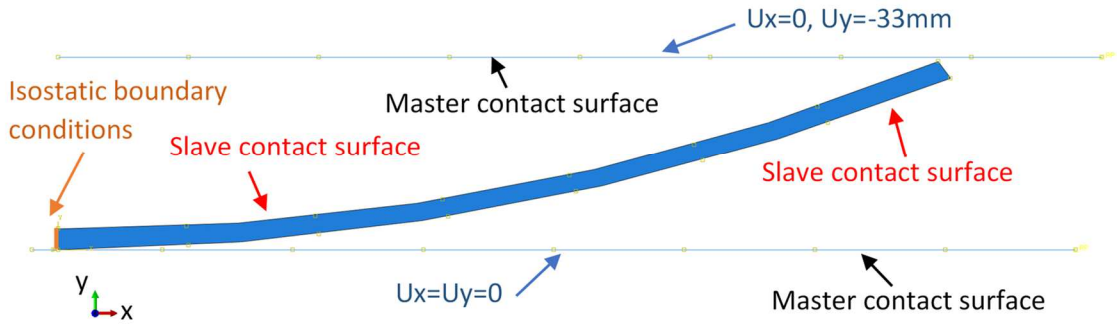

Figure 16: Boundary conditions and loading applied on the numerical model

A 2D model, using quadrangular elements with quadratic interpolation (CPS8), is carried out. The mesh is made by the "Structured" technique. The discretization of the curved geometry was carried out by 200 nodes in the length of the sample and 5 nodes in the thickness of the coating, to give a total number of 1000 elements.

Figure 17 presents the numerical results of the stresses calculated from the Tresca criterion. The result show that maximum stress around 4-5 MPa has been calculated in the coating. This value can be considered as the value of stress (elastic stress) present in the coating in service. These stress values are consistent with the stress levels estimated previously (Figure 12),

between 4 and 9 MPa at the steel/FBE interface (function of temperature and pressure cases).

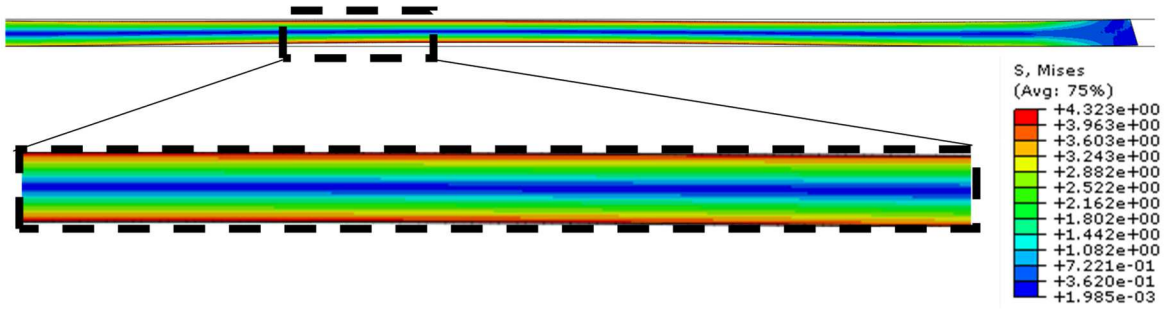

Figure 17: Isovalues of the stress values in the radial and longitudinal directions and Tresca criteria (MPa) after recovery of the sample (mechanical loading)

4.2. Model 2 based on thermal loading

In the assumption that the stresses come mainly from the coating process, a second model has been developed directly inspired from the process stage. The idea is to apply a temperature on the upper surface of the sample in order to reproduce the thermal gradient allowing a return to a plan position of the sample. In this case, numerical model is based on a deformable part (coating curved) and only one rigid part (bearing surface of the sample – blue line Figure 17). Contact properties are identical to model 1 (model based on mechanical approach). Isostatic boundary conditions are imposed as shown in Figure 17. A temperature is imposed (T = 55°C – hot temperature value at the end of the coating process) on the upper surface of the sample while the lower surface is maintained at room temperature (T = 20°C).

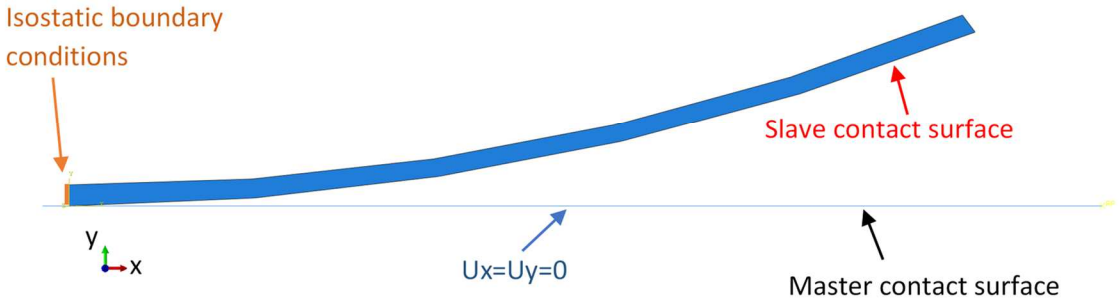

Figure 18: Boundary conditions and loading applied on the numerical model

A 2D thermomechanical model, using quadrangular elements with quadratic interpolation (CPE8RT), is carried out. The mesh is made by the "Structured" technique with an element size similar to the previous model.

Figure 19 presents the numerical results of the stresses calculated from the Tresca criterion. The result show that maximum stress around 4 MPa has been calculated in the coating. This value confirms the previous results on the order of magnitude of the residual stress in the coating.

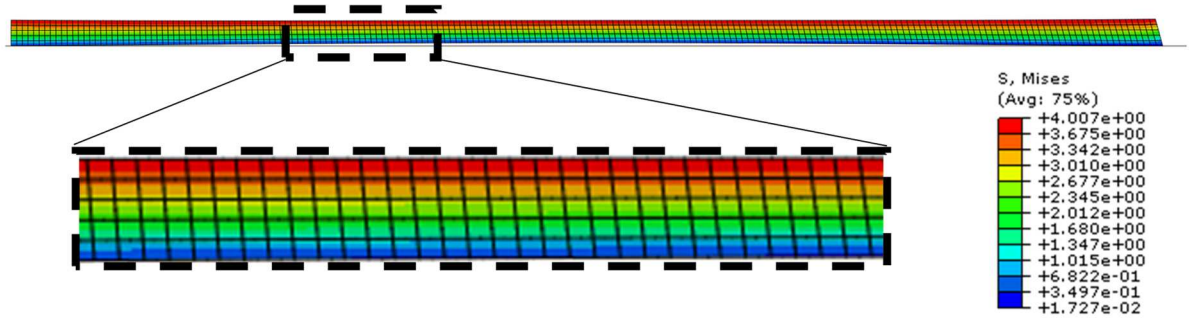

Figure 19: Isovalues of the stress values in the radial and longitudinal directions and Tresca criteria (MPa) after recovery of the sample (thermal loading)

5. Conclusion

This study has shown that the pressure and the temperature are favourable to decrease the shear stress at the different interfaces present in the three-layers coating. In service, the interfacial stresses are therefore generally greater than the residual stresses after storage of the coated tube at ambient temperature (except at PE/FBE interface, in the case where the temperature of the gas is +60°C). When the gas is injected at a low temperature (-20°C), which is particularly the case at the exit of the compressor stations, the highest stresses are observed at PE/FBE interface. On the other hand, when the gas is injected at a higher temperature (+15°C or +60°C), which is the case on most of the transportation network, the highest stresses are at the steel/FBE interface which is therefore the most critical interface.

Furthermore, an industrial feedback (coating sample of three-layer coating cutted in the

longitudinal direction of the pipe) has allowed us to estimate that the stresses in the coating are between 4 and 5 MPa for the three-layers coating. These values are consistent with the stress levels estimated, between 4 and 9 MPa at the steel/FBE interface, obtained by successive modelling of the different steps of pipeline life (coating process, pipeline storage and service conditions). Moreover, this feedback helps to validate the numerical model developed in this project due to the small difference observed between these numerical results.

However, this study can not fully explain the debonding cases observed occasionally between the three-layers coating and the steel cylinder. One possible cause could be the loss of interface performance due the combination with aging phenomena, especially with the water diffusion from the soils across the polymer coating up to the steel/FBE interface.

Acknowledgment

Financial support by the GDF Suez, DRI-CRIGEN, Pôle Mécanique, Matériaux, Intégrité des structures is gratefully acknowledged.

References

[1] L. Zardasti, N. Yahaya, A. Valipour, A. Safuan A. Rashid, N. Md Noor, Review on the identification of reputation loss indicators in an onshore pipeline explosion event, Journal of Loss Prevention in the Process Industries 48 (2017) 71–86.

[2] H.R. Vanaei, A. Eslami, A. Egbewande, A review on pipeline corrosion, in-line inspection (ILI), and corrosion growth rate models, International Journal of Pressure Vessels and Piping 149 (2017) 43–54.

[3] Y. Sahraoui, R. Khelif, A. Chateauneuf, Maintenance planning under imperfect inspections of corroded pipelines , International Journal of Pressure Vessels and Piping 104 (2013) 76–82.

[4] C.I. Ossai, B. Boswell, I.J. Davies, Pipeline failures in corrosive environments – A conceptual analysis of trends and effects, Engineering Failure Analysis53 (2015) 36–58.

[5] L. Zardasti, N. Yahaya, A. Valipour, A. Safuan A. Rashid, N. Md Noor, Review on the identification of reputation loss indicators in an onshore pipeline explosion event , Journal of Loss Prevention in the Process Industries 48 (2017) 71–86.

[6] H.A. Kishawy, H.A. Gabbar, Review of pipeline integrity management practices, International Journal of

Pressure Vessels and Piping, 87 (2010) 373–380.
[7] F. Ubaid, A.B. Radwan, N. Naeem, , R.A. Shakoor, Z. Ahmad, M.F. Montemor, R. Kahraman, A.M. Abdullah, Ahmed Soliman, Multifunctional self-healing polymeric nanocomposite coatings for corrosion inhibition of steel, Surface and Coatings Technology, 372 (2019) 121-133.
[8] A. López-Ortega, R. Bayóna, J.L. Arana, Evaluation of protective coatings for offshore applications. Corrosion and tribocorrosion behavior in synthetic seawater, Surface and Coatings Technology, 349 (2018) 1083-1097.
[9] S.M. Hanetho, I. Kaus, A. Bouzga, C. Simon, T. Grande, M.A. Einarsrud, Synthesis and characterization of hybrid aminopropyl silane-based coatings on stainless steel substrates, Surface and Coatings Technology, 238 (2014) 1-8.
[10] M. Barletta, F. Trovalusci, A. Gisario, S. Venettacci, New ways to the manufacturing of pigmented multi-layer protective coatings, Surface and Coatings Technology, 232 (2013) 860-867.
[11] X. Chen, X.G. Li, C.W. Du, Y.F. Cheng, Effect of cathodic protection on corrosion of pipeline steel under disbonded coating, Corrosion Science 51 (2009) 2242–2245.
[12] G.M. Harris, A. Lorenz, New coatings for the corrosion protection of steel pipelines and pilings in severely aggressive environments, Corrosion Science 35 (1993) 1417–1423..
[13].G.P. Guidetti, G.L. Rigosi, R. Marzola, The use of polypropylene in pipeline coatings, Progress in Organic Coatings, 27 (1996) 79–85.
[14].V. Ashworth, C.G. Googan, Cathodic Protection - Theory and Practice, Ellis Horw, Chichester, 1993.
[15] O. Vestrum, M. Langseth, T. Børvik, Finite element modeling of porous polymer pipeline coating using X-ray micro computed tomography, Composites Part B: Engineering 172 (2019) 406-415.
[16] M.R. Tchoquessi-Diodjo, Y. Joliff, L. Belec, E. Aragon, F.X. Perrin, M. Bonnaudet, L. Lanarde, Numerical modeling of stresses relaxation phenomena in the complex assembly steel pipe/three layers polyethylene coating, Progress in Organic Coatings 104 (2017) 152–160.
[17] G. Portesan, J. Taves, G. Guidetti, Cases of Massive Disbondment with Three-Layer PE Pipeline Coatings, Cathodic Protection and Associated Coatings, CEFRACOR, EFC Event nr 254, June 6–7, Aix-en-Provence, France, 2002.
[18] M. Roche, D. Melot, G. Paugam, Recent experience with pipeline coating failures., Journal of Protective Coatings & Linings (2006).
[19] K.K. Tandon, G.V. Swamy, G. Saha, Performance of three layer polyethylene coating on a cross country pipeline a - case study, 14th International Conference on Pipeline Protection, BHR Group (Ed.), October 29-31, Barcelona, Spain, 2001.
[20] E. Legghe, Y. Joliff, L. Belec, E. Aragon, A. Margaillan, Computational analysis of internal stresses generated during the manufacturing process of a monolayer or three-layer pipeline coating, Computational Materials Science. 48 (2010) 360–365.
[21].L.L. Shaw, Thermal residual stresses in plates and coatings composed of multi-layered and functionally graded materials, Composites Part B: Engineering 29 (1998) 199-210.
[22].C. H. Hsueh, S. Lee, Modeling of elastic thermal stresses in two materials joined by a graded layer, Composites Part B: Engineering 34 (2003) 747-752.
[23].N.H. Zhang, J.Z. Chen, An alternative model for elastic thermal stresses in two materials joined by a graded

layer, Composites Part B: Engineering 41 (2010) 375-379.
[24] F. Moleiro, V.M. Franco Correia, A.L. Araújo, C.M. Mota Soares, A.J.M. Ferreira, J.N. Reddy, Deformations and stresses of multilayered plates with embedded functionally graded material layers using a layerwise mixed model, Composites Part B: Engineering 156 (2019) 274-291.
[25] C.T. Chuang, C.K. Chao, R.C. Chang, K.Y. Chu, Effects of internal stresses on the mechanical properties of deposition thin films, Journal of Materials Processing Technology 201 (2008) 770–774.
[26] B.T.A. Chang, H.-J. Sue, H. Jiang, B. Browning, D. Wong, H. Pham, S. Guo, A. Kehr, M. Mallozzi, W. Snider, A. Siegmund, Integrity of 3LPE pipeline coatings: residual stresses and adhesion degradation, 7th International Pipeline Conference, Calgary, Canada, 2008.
[27] B.T.A. Chang, H. Jiang, H.-J. Sue, S. Guo, G. StJean, H. Pham, D. Wong, A. Kehr, M. Mallozzi, K.H. Lo, Disbondment mechanism of 3LPE pipeline coatings, 17th International conference on Pipeline Protection, Edinburgh, Scotland, 2007.
[28] J. Bouchet, A.A. Roche, P. Hamelin, Internal stresses, Young's modulus and practical adhesion of organic coatings applied onto 5754 aluminium alloy, Thin Solid Films 355-356 (1999) 270–276.
[29] S. Guo, K.H. Lo, B.T.A. Chang, Corrosion Nace. International, houston, USA, 2011.
[30] M. Piens, H. De Deurwaerder, Effect of coating stress on adherence and on corrosion prevention, Progress in Organic Coatings 43 (2001) 18–24.
[31] D.Y. Perera, On adhesion and stress in organic coatings, Progress in Organic Coatings 28 (1996) 21–23.
[32] K. SATO, The internal stress of coating films, Progress in Organic Coatings, 8 (1980) 143–160.
[33] E. Legghe, Y. Joliff, L. Belec, E. Aragon, Computational analysis of a three-layer pipeline coating: Internal stresses generated during the manufacturing process, Computational Materials Science, 50 (2011) 1533–1542.
[34] M.R. Tchoquessi-Diodjo, Y. Joliff, L. Belec, E. Aragon, F.X. Perrin, M. Bonnaudet, L. Lanarde, M. Meyer, Computational modeling of quenching step of a coated steel pipe with thermo-elastic, thermo-plastic and thermo-viscoelastic models: Impact of masking tape at tube ends, Computational Materials Science 85 (2014) 67–79.
[35] M.R. Tchoquessi-Diodjo, L. Belec, E. Aragon, F.X. Perrin, M. Bonnaudet, L. Lanarde, M. Meyer, Y. Joliff, Numerical modelling of pipe internal stresses induced during the coating process – Influence of pipe geometric characteristics on stress state, Materials & Design 52 (2013) 429–440.
[36] M. Fraldi, A. Cutolo, L. Esposito, G. Perrella, M.G.P. Carbone, L.Sansone, G. Scherillo, G. Mensitieri, Delamination onset and design criteria of multilayer flexible packaging under high pressure treatments, Innovative Food Science & Emerging Technologies 23 (2014) 39–53.
[37] E. Shashi Menon, Pipeline Planning and Construction Field Manual, 1st editio, Oxford, 2011.
[38].Dassault Systèmes. Abaqus 2016 Analysis User's Guide; 2015.
[39] M.R. Tchoquessi-Diodjo, Amélioration de l'adhésion de revêtements épais sur acier : étude expérimentale et numérique, PhD Thesis, Université de Toulon, 2013.
[40] F. Cardarelli, Materials handbook – a concise desktop reference (2nd ed.), Springer-Verlag, London Limited (2008).
[41] M.J. Peet, H.S. Hasan, H.K.D.H. Bhadeshia, Prediction of thermal conductivity of steel International, Journal of Heat and Mass Transfer, 54 (2011) 2602–2608.
[42] J. Zhu, H. Xie, Z. Hu, P. Chen, Q. Zhang, Residual stress in thermal spray coatings measured by curvature

based on 3D digitalimage correlation technique, Surface and Coatings Technology 206 (2011) 1396–1402.
[43] E. Legghe, E. Aragon, L. Belec, A. Margaillan, D. Melot, . Correlation between water diffusion and adhesion loss: Study of an epoxy primer on steel, . Progress in Organic coatings. 66 (2009) 276–280.
.